Chapter 13
Fundamentals

Etsuo Akiba

Abstract This chapter describes fundamental knowledge indispensable for hydride-based hydrogen storage, including the physical and chemical properties of hydrogen, phase diagrams of metal-hydrogen systems, hydrogen-material interaction, as well as thermodynamic stability and the reaction kinetics of hydrides.

Keywords Hydrogen · Phase diagram · Hydrogen-material interaction · Thermodynamics · Miedema's rule · Kinetics · Hydrogen storage

13.1 Physical and Chemical Properties of Hydrogen

Hydrogen is an element with the chemical symbol H and atomic number 1 and is the lightest element in the periodic table. Hydrogen was first produced from metals and acids in the early sixteenth century. In eighteenth century, Henry Cavendish recognized that hydrogen gas was a discrete substance.

Hydrogen is the most abundant chemical element in the universe, making up 75 % of normal matter by mass and over 90 % by number of atoms (excluding dark matter and dark energy). On the earth, hydrogen gas usually exists in diatomic molecule form as H_2. Some physical properties of hydrogen are shown in Table 13.1.

There exist two different spin isomers of hydrogen diatomic molecules, orthohydrogen and parahydrogen. They differ by the relative spin of their nuclei. In the orthohydrogen form, the spins of the two protons are parallel, while in the parahydrogen form the spins are antiparallel. At standard temperature and pressure, hydrogen gas contains about 25 % of the para form and 75 % of the ortho form, also known as the "normal form." The equilibrium ratio of orthohydrogen to parahydrogen depends on temperature. At very low temperatures, the equilibrium

E. Akiba (✉)
Department of Mechanical Engineering, Faculty of Engineering, Kyushu University, Fukuoka, Japan
e-mail: e.akiba@mech.kyushu-u.ac.jp

© Springer Japan 2016

K. Sasaki et al. (eds.), *Hydrogen Energy Engineering*,
Green Energy and Technology, DOI 10.1007/978-4-431-56042-5_13

Table 13.1 Some physical properties of hydrogen, especially useful for applications

Molecular weight	2.016
Boiling point	−252.0 °C
Melting point	−259.1 °C
Density (air = 1)	0.0695
Critical pressure	13.0 bar
Critical temperature	−240.0 °C
Density of liquid (boiling point)	70.8 kg/m^3
Density of gas (20 °C, 1 bar)	0.083764 kg/m^3
Thermal conductivity (20 °C, 1 bar)	1.897 mW/cm·K

state is composed almost 100 % of the para form. The conversion from ortho to para is exothermic and produces enough heat to evaporate some of the hydrogen in the liquid phase, leading to loss of liquefied material. For liquefaction of hydrogen, conversion from ortho to para form is accelerated using catalyst to prevent evaporation of produced liquid hydrogen.

Hydrogen has three isotopes, denoted as ^{1}H, ^{2}H, and ^{3}H. ^{1}H is the most common hydrogen isotope with an abundance of more than 99.98 %. Because the nucleus of this isotope consists of a single proton and no neutron, it is given the formal name protium but this is rarely used. ^{2}H is known as deuterium and contains one proton and one neutron in its nucleus. ^{3}H is known as tritium and contains one proton and two neutrons in its nucleus. It is radioactive, decaying into ^{3}He through beta decay, with a half-life of 12.32 years. The symbols D and T for isotopes of hydrogen instead of ^{2}H and ^{3}H are sometimes used for deuterium and tritium, respectively.

Hydrogen gas forms explosive mixtures with air in 4–75 % concentration by volume. Detecting low concentration hydrogen is a significantly important technique with high accuracy. The flame of hydrogen burning is nearly invisible. The enthalpy of combustion for hydrogen is −286 kJ/mol H_2.

Hydrogen forms hydrides with various elements but takes negative, neutral, and positive characters depending on elements to form hydrides. Details of hydride will be discussed later in this book.

13.2 Phase Diagram of Metal-Hydrogen Systems

Thermodynamic factors determine the major features of the metal-hydrogen systems. An understanding of the thermodynamic properties of these systems is very important, especially for certain kinds of application such as hydrogen transportation and storage, heat pumps and thermal storage, because their performance in such applications is largely determined by thermodynamic parameters. This section will focus on the practical aspects of the thermodynamic properties of the metal-hydrogen systems. The corresponding theoretical aspects of these properties

have been described in detail by Flanagan and Oates [1] and by Griessen and Riesterer [2].

The equilibrium relationship between metal and hydrogen is illustrated by means of pressure-composition-temperature (*p*-*c*-*t*) isotherms, as shown in the example given in Fig. 13.1. When hydrogen gas is introduced into the system, it dissolves in the lattice of the metal and forms a solid solution. This takes place over the region shown by AB in Fig. 13.1. Hydrides formed from metals and hydrogen are chemical compounds and, therefore, by using the Gibbs' phase rule

$$f = c - p + 2 \tag{13.1}$$

the degree of freedom of the system, *f*, is unity in the region where the metal (in practice the hydrogen solid-solution phase) is in equilibrium with its hydride and gaseous hydrogen (in this case the number of components *c* is 2, and the number of phases *p* is 3). This means that, for a given temperature, the hydrogen equilibrium pressure is constant in the two-phase region, shown as the plateau section, BC, in the isotherm given in Fig. 13.1. These characteristics can be used advantageously in "thermodynamic machines" and hydrogen-storage systems, because during the hydrogenation and dehydrogenation processes the hydrogen pressure remains constant. However, in reality the plateau region is not flat but shows a more or less sloping curve and the hydrogen absorption and desorption pressures differ.

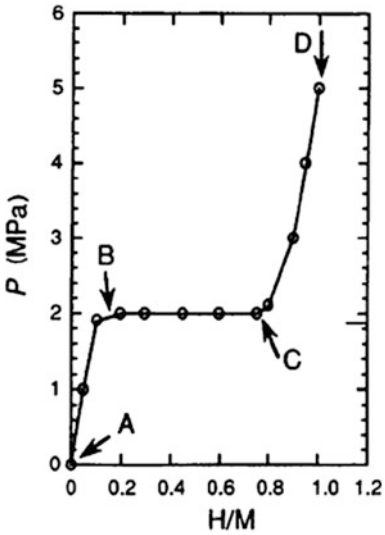

Fig. 13.1 Pressure-composition (*p*-*c*) isotherm

13.3 Hydrogen-Material Interaction

The principle of formation of transition metal hydrides is essentially the formation of a metallic bond. Transition metals belonging to groups 3 through 5 and Pd form stable binary hydrides. The radius of these metals is in the range 123–200 pm but that of hydrogen ranges 35–40 pm. Therefore, hydrogen can occupy the interstitial site of the metallic sublattice. However, even though the hydrogen atom is small, 20–30 % of volume expansion usually can be observed after metal hydride is formed. The interaction of hydrogen materials of most intermetallic compounds that form stable hydrides is similar to binary hydrides.

In the case of alkali and alkaline earth elements with low electropositivity, the hydride consists of the cation of these metals and the anion of hydrogen (H^-). For example, NaH has the same structure as NaCl. Mg and Al are most promising hydride forming elements because they are rich in the earth's crust and form hydrides with more than 7 wt% of gravimetric capacity. The bonding state of Mg and Al hydrides has been intensively studied and it has been reported that both hydrides have an intermediate nature of ionic and covalent bonding, but not bonding of a metallic (interstitial) nature.

In the electronic structure of transition metal hydrides, hydrogen gives an electron to the d-band to make a bonding state. In case of alloys with Mg and rare earth elements, the energy band of these elements is far too low to form a bonding state with hydrogen. Hydrogen will bond with the d-band of transition metals to form an alloy, just below the Fermi level. Figure 13.2 shows a schematic drawing of the electronic structure of hydrides of intermetallic compounds.

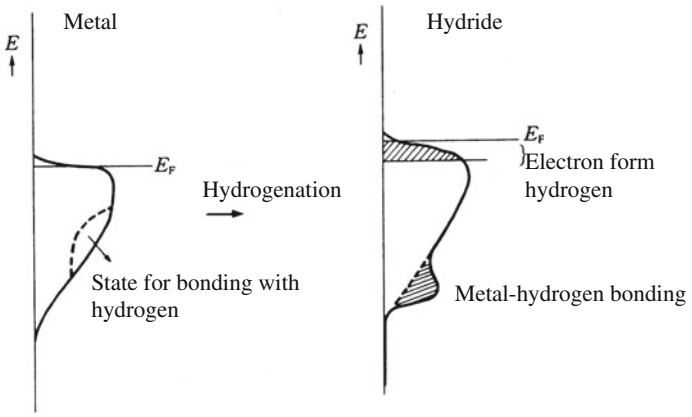

Fig. 13.2 Schematic drawing of electronic structure of hydrides of intermetallic compounds

13.4 Enthalpy of Hydride Formation and Equilibrium Pressure

The enthalpy (heat) of hydride formation is a very important parameter of metal-hydrogen systems, particularly with applications of "thermodynamic machines," where the enthalpy of hydride determines the power and efficiency. The enthalpy of hydride formation, ΔH, is usually calculated from the variation in equilibrium pressure, P_{H2} with the temperature T by using

$$\ln P_{H2} = \Delta H/RT - \Delta S/R \tag{13.2}$$

The plot of the hydrogen equilibrium pressure versus the reciprocal of the absolute temperature, $1/T$, is called a van't Hoff plot, where the slope and intercept with the y axis give the enthalpy change in hydride formation, ΔH, and the entropy change of hydride forming, ΔS, respectively. Figure 13.3 shows the van't Hoff plots for a selected number of intermetallic compound-hydrogen systems, while in Fig. 13.4, the van't Hoff plots for the two plateau regions in Fig. 13.5 are presented. The equilibrium desorption pressures at hydrogen-to-metal ratios H/M of 0.25 and 0.7 were plotted and the slopes of these plots give the different enthalpies of decomposition of the $LaNi_5H_6$ and $LaNi_5H_3$ phases (−32.7 and −26.8 kJ/mol H_2, respectively).

The change in Gibbs free energy of hydride formation can be described by

$$\Delta G = \Delta H - T\Delta S \tag{13.3}$$

or

$$\Delta G = -RT \ln K = RT \ln P_{H2} \tag{13.4}$$

and Eq. 13.2 can be derived directly from these two equations.

Equilibrium pressures of metal-hydrogen systems can be determined from p-c isotherms like that shown in Fig. 13.1. However, the observed isotherms may have a sloping plateau, and exhibit "sorption hysteresis" (see Fig. 13.5). In

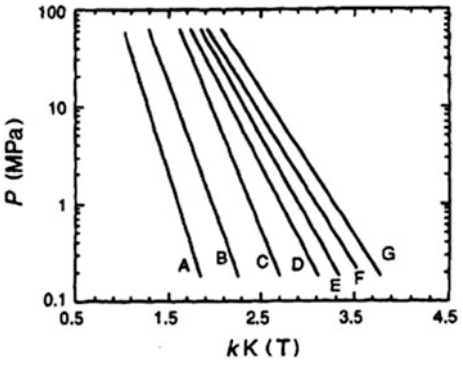

Fig. 13.3 van't Hoff plots for selected alloy-hydrogen systems: A Mg_2Ni; B $LaNi_4Al$; C $ZrMn_2$; D $LaNi_{4.8}Al_{0.2}$; E $LaNi_5$; F TiFe; G $Ti_{1.2}Mn_{1.8}$

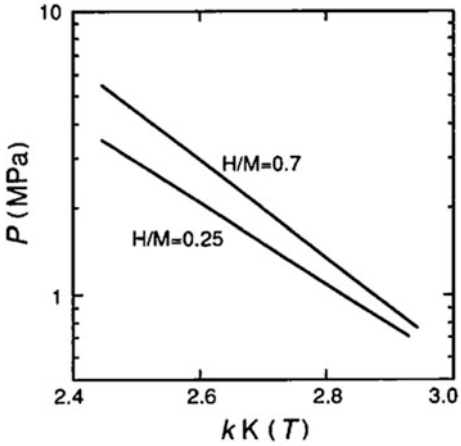

Fig. 13.4 van't Hoff plots for the $LaNi_5$-H_2 system for the two-plateau region

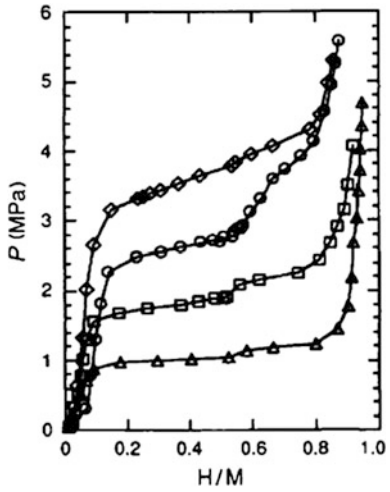

Fig. 13.5 Pressure-composition isotherm of the $LaNi_5$-H_2 system: at 353 K (*open triangle*), 373 K (*open square*), and 393 K (desorption, *open circle*; absorption, *open diamond*)

addition, it has been found that factors such as the preparative method used to make the intermetallic compounds, the variation in the ratio of the component metals, the annealing conditions, the procedures used for the activation process, and the number of hydrogenation–dehydrogenation cycles that are carried out influence the equilibrium hydrogen pressure [3].

In general, the difference in standard entropy between an alloy and its hydride is very small and is on the order of 10 J/(mol K). The change in entropy with hydride formation is mainly provided by the loss of the standard entropy of hydrogen gas

(130.858 J/(mol K) at 298 K), which means that ΔS can be assumed to be a constant and does not depend on the nature of the intermetallic compound [4]. Equation 13.5 can be used instead of Eq. 13.2, where C ($-\Delta S/R$) is a constant and does not depend upon the intermetallic compound. A sufficient number of sets of temperatures and equilibrium pressures are needed for calculation of the enthalpy of hydride formation when using Eq. 13.2. However, by using Eq. 13.5, only a pair of the temperature and equilibrium hydrogen pressure values is required to approximately calculate the enthalpy of formation. This method is very convenient to obtain a first impression of the thermodynamic properties of the ternary hydrides. However, when using Eq. 13.2 the experimental conditions used during the measurements have to be carefully monitored, because various factors may influence these values.

$$\ln P_{H2} = \Delta H/RT + C \tag{13.5}$$

Accurate data for the enthalpy of hydride formation can be obtained using calorimetry. However, this method requires very sensitive measurements to be made and only relatively few studies have been reported [5–9]. A typical apparatus that is used for measurements of the enthalpy of formation by this technique is a Calvet-type calorimeter with twin sample cells [5]. This apparatus uses a high-pressure hydrogen supply and is able to measure the amount of reacted hydrogen. Table 13.2 shows the enthalpy of hydride formation of some typical intermetallic compounds. Although this data has been mainly derived from the van't Hoff plots of the hydrogen equilibrium pressure, of the type shown in Fig. 13.3, some results obtained from calorimetric measurements are also listed for a few of the systems.

Table 13.2 Thermodynamic properties of some typical intermetallic-hydrogen systems

IMC (M)	Amount of hydrogen. x in MH_x	Hydrogen equilibrium pressure, P (T) (MPa (K))	Enthalpy of hydride formation, H (kJ/mol H_2)	Reference
$LaNi_5$[a]	6.3	0.097 (285)	−31.83 ± 0.09	Murray et al. [10]
$LaNi_5$	6	0.37 (313)	−31.2	Buschow and van Mal [11]
$LaNi_{4.8}Al_{0.2}$	6	0.2 (323)	−35	Mendelsohn [12]
$LaNi_4Al$	4	0.2 (453)	−53	Mendelsohn [12]
$MmNi_5$[b]	6.3	1.3 (293)	−30	Osumi et al. [13]
TiFe	2	0.73 (313)	−28.1 ($x < 1.04$)	Reilly and Wiswall [14]
TiCo	1.4	0.101 (403)	−57.7 ($x < 0.6$)	Osumi et al. [15]
$Ti_{1.2}Mn_{1.8}$	2.47	0.7 (293)	−28	Gamo et al. [16]

(continued)

Table 13.2 (continued)

IMC (M)	Amount of hydrogen. x in MH_x	Hydrogen equilibrium pressure, P (T) (MPa (K))	Enthalpy of hydride formation, H (kJ/mol H_2)	Reference
$ZrMn_2$	3.46	0.23 (374)	−44.4	Ishido et al. [17]
ZrV_2	5.5	10^{-7} (323)	−202	Shaltiel et al. [18]
Mg[c]	2	0.92 (638)	−76.15 ± 9.2	Chase et al. [19]
Mg_2Ni	4	1.15 (633)	−62.7	Nomura et al. [20]
$CaNi_5$[a]	6	0.077 (313)	−33.1 ± 0.5 ($1.1 < x < 2.0$)	Murray et al. [6]
$CaNi_5$	6.2	0.08 (313)	−33.5 ($1.1 < x < 4.5$)	Sandrock et al. [21]

[a]Data obtained using calorimetry; [b]Mischmetal (Mm); [c]an average of the data obtained using both calorimetry and van't Hoff plots

13.5 The Stability of Intermetallic Compound Hydrides

Because the stability of hydrides is such an important property, empirical rules have been proposed to predict the stability of a given intermetallic compound-hydrogen system. Miedema's rule of reversed stability is the most popular one [22], which proposes the following relationship between the hydride and alloy stabilities:

$$\Delta H(\mathrm{AB}_n\mathrm{H}_{2m}) = \Delta H(\mathrm{AH}_m) + \Delta H(\mathrm{B}_n\mathrm{H}_m) - \Delta H(\mathrm{AB}_n) \tag{13.6}$$

In this model, the enthalpy effects are considered to arise from the effective areas of contact between the component elements.

In the simplest case, the enthalpy of formation of a hydride of intermetallic compound is the difference between the sum of the hydride formation enthalpies of the two component metals and the intermetallic compound formation enthalpy. Generally, the first term on the right-hand side of Eq. 13.6 is negative and has the largest absolute value, whereas the second term on this side is small and may be positive. Therefore, the sum of the first and second terms has an almost constant value for a given class of intermetallic compound system. This means that if the third term on the right-hand side of this equation becomes more negative (equivalent to a *more stable intermetallic compound*), the left-hand side becomes more positive (equivalent to a *more unstable intermetallic compound hydride*). In the case of $LaNi_5$, the relationship becomes

$$\Delta H(\mathrm{LaNi_5H_6}) = \Delta H(\mathrm{LaH_3}) + \Delta H(\mathrm{Ni_5H_3}) - \Delta H(\mathrm{LaNi_5}) \tag{13.7}$$

The values for each term on the right-hand side of this equation are −252, +4, and −168 kJ/(mol alloy), respectively, which then gives a value for the formation enthalpy of the intermetallic compound hydride as −80 kJ/(mol alloy) [viz. −27 kJ/(mol H_2)]. This agrees well with the observed value of −32 kJ/(mol H_2) [22]. $LaCo_5$ belongs to the same series of alloys as $LaNi_5$, but is less stable than the latter. Calculations show that $\Delta H(LaCo_5)$ is −50 kJ/(mol H_2) [22], and the hydride of $LaCo_5$ is found to be more stable than that formed with $LaNi_5$, clearly showing that these AB_5-type hydrides obey the rule of reversed stability. A similar relationship is also found in the Mg_2XH_y (where X = Fe, Co or Ni) systems. Mg_2Fe and Mg_2Co alloys do not actually exist but their hydrides were prepared using mechanical alloying or sintering techniques [23, 24]. Therefore, it can be assumed that Mg_2Fe and Mg_2Co alloys are less stable than the Mg_2Ni alloy. The observed hydrogen equilibrium pressures of Mg_2FeH_x and Mg_2CoH_x are both lower than that of Mg_2NiH_x when measured at the same temperature [23, 24]. Therefore, the hydrides of Mg_2Fe and Mg_2Co are more stable than that of Mg_2Ni. This means that in these systems *less stable alloys form more stable hydrides*.

13.6 Reaction Kinetics

The direct reactions between intermetallic compounds and gaseous hydrogen are solid-phase gas-phase reactions, which differ in some aspects from homogeneous reactions. First, the presence of "boundaries" influences the reaction kinetics and mechanisms.

Hydrogen gas exists only at the surface of the intermetallic compound [25]; a hydrogen molecule (H_2) is first adsorbed on the surface, where it is dissociated into individual hydrogen atoms (H). Then the hydrogen atoms diffuse into the bulk of the intermetallic compound and form the hydride (see Fig. 13.6). Therefore, the surface (one of the "boundaries") plays an important role in the whole reaction. As previously mentioned, intermetallic compounds consist of small particles, and the reaction proceeds independently inside each of the particles. The hydrogen atoms on the surface diffuse into the particles to react with the metal atoms, and in some cases, the reaction is controlled by diffusion through the boundary that exists between the hydride layers and the metallic atoms [17, 26].

Theoretically, a homogeneous reaction is initiated in the same manner at any atom because the molecules are moving vigorously in both the liquid and the gas phases. In contrast, a solid-phase-gas-phase reaction generally starts in a particular part of the solid where reaction nuclei can readily form such as grain boundaries, crystal defects, and impurities. All of the atoms of the solid do not contribute equally to the reaction because atoms are fixed in given positions. This is a second important feature of the solid-phase-gas-phase reaction. Therefore, in many cases, a simple kinetic equation cannot be used to describe the reaction. The method of

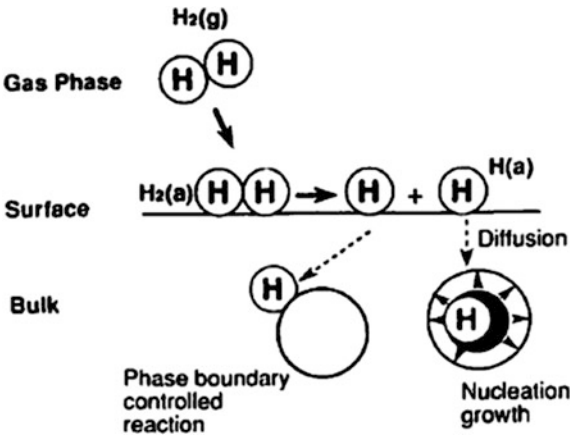

Fig. 13.6 Schematic representation of the reaction that occurs between an alloy and gaseous hydrogen

preparation, activation procedures, and the past history of the intermetallic compound sample significantly influence the reaction kinetics, because they determine the particle size, the number of defects, and the size and nature of any precipitate species in the grain boundaries [27, 28]. To date, there have been only a few studies of the relationship between the microstructure of intermetallic compounds and the reaction kinetics, even though the microstructures are known to determine the reaction kinetics and mechanisms of these materials.

As previously described, activated intermetallic compounds exist in the form of very fine powders and have low thermal-conductivity values. Efficient removal of the reaction heat is therefore essential, otherwise the reaction rate would be largely determined by heat-transfer processes. However, in practice the thermal conductivities of the reactors used for hydrogenation are not high enough to achieve this, and therefore, the reaction rates are largely controlled by heat transfer in almost all cases [29]. Currently, the observed reaction kinetics are overall reaction rates, which include contributions from both the intrinsic reaction rate and the heat-transfer rate, and are greatly influenced by the microstructures of the intermetallic compounds. In this section, the methods of measurement, analysis of the reaction rates, and some of the experimental results that have been obtained, will be discussed.

In solid-state reactions, the fraction of a material that has reacted is used as a parameter for representing the change in the concentration of that substance in the original solid. If the parameter "α" represents the ratio of the amount of reacted material to the total, i.e., original amount of material, the solid-state rate equations can be generally expressed by

$$F(\alpha) = kt \tag{13.8}$$

where k and t are the rate constant and the reaction time, respectively. Historically, the rates of gas-phase-solid-phase reactions have been extensively studied using the gravimetric method, for decomposition reactions of inorganic salts, such as carbonates and oxalates. The parameter α is very convenient for the analysis of such data, because it can be easily calculated from the weight changes that are observed.

Table 13.3 gives various rate equations, both observed and theoretically derived, that have been used to study solid-phase-gas-phase reactions. Usually, the reaction mechanism is analyzed by comparing the observed rate with those given by the equations in this table [30].

Hancock and Sharp [31] have proposed a very convenient method for the analysis of a reaction mechanism. Equation 13.9, shown in Table 13.3, is known as the Avrarni–Erofeev equation and is given as

$$\alpha = 1 - \exp(-Bt^m) \tag{13.9}$$

where m is used instead of l. From Eq. 13.9, the following can be derived:

$$-\ln[\ln(1-\alpha)] = \ln B + m \ln t \tag{13.10}$$

where B and m are constants. It has been found that all of the equations listed in Table 13.3 can also be expressed by Eq. 13.10 for $0.15 < \alpha < 0.50$. By using Table 13.4, in conjunction with Eq. 13.10, the rate equation which best fits the observed data can be found for the appropriate value of m. This procedure is a very effective one for the analysis of systems that show an induction period, and for those in which the exact starting time of the reaction cannot be determined.

The method of Hancock and Sharp [31] is suitable for the study of the decomposition of intermetallic compound hydrides, in particular when carried out

Table 13.3 Selection of various rate equations that have been used to analyze gas-solid phase reactions

Type of reaction	Equation
Branching reaction	$dx/dt = A + B\,\alpha^n$
Nucleation and growth processes	$\alpha = kt^n$ $\alpha = 1 - \exp(-B\,t')$
Autocatalytic reaction	$\ln[\alpha/(1-\alpha) = k(t - t_c)$
Order of reaction	$\alpha = kt$ $dx/dt = k(1-\alpha)$
Phase-boundary-controlled reaction	$1 - (1-\alpha)^{1/n} = kt/r_0$ $1 - (1-\alpha)^{1/3} = kt/r_0$ $1 - (1-\alpha)^{1/2} = kt/r_0$
Diffusion-controlled contracting reaction	$[1 - (1-\alpha)^{1/3}]^2 = kt/r_0$ $(1-\alpha)\ln(1-\alpha) + \alpha = kt$

Table 13.4 Values of m that have been used in Eq. 13.10, and the corresponding rate equations

Rate equation	m
$\alpha^2 = kt$	0.62
$(1-\alpha)\ln(1-\alpha)+\alpha = kt$	0.57
$[1-(1-\alpha)^{1/3}]^2 = kt$	0.54
$1-2\alpha/3-(1-\alpha)^{2/3} = kt$	0.57
$-\ln(1-\alpha) = kt$	1.00
$1-(1-\alpha)^{1/2} = kt$	1.11
$1-(1-\alpha)^{1/3} = kt$	1.07
$\alpha = kt$	1.24
$[-\ln(1-\alpha)]^{1/2} = kt$	2.00
$[-\ln(1-\alpha)]^{1/3} = kt$	3.00

under vacuum, or in the absence of hydrogen. However, hydrogen gas must be present during hydride formation, and in such cases, the hydrogen pressure is an important factor in the determination of the reaction kinetics [25]. In general, three types of pressure dependence are expected. The effective hydrogen pressure, i.e., the "driving force of the reaction," is not the partial hydrogen pressure but is the difference between the ambient hydrogen pressure and the hydrogen equilibrium pressure, as follows:

$$\Delta P = P_{\mathrm{H2}} - P_{\mathrm{e}} \tag{13.11}$$

where P_{H2} and P_{e} are the hydrogen pressure in the system, and the hydrogen equilibrium pressure at the reaction temperature, respectively. Three typical rate equations can be derived:

$$\mathrm{d}n/\mathrm{d}t = A\Delta P \tag{13.12}$$

$$\mathrm{d}n/\mathrm{d}t = A\Delta P^{1/2} \tag{13.13}$$

$$\mathrm{d}n/\mathrm{d}t = A\Delta P^{o} \tag{13.14}$$

where n represents the fraction of the alloy that has reacted, and A is a constant. The reaction scheme for hydride formation is shown schematically in Fig. 13.6. The relationship between the hydrogen pressure and the concentration of the hydrogen atoms is given by Sievert's law

$$[H(\mathrm{a})] = K\mathrm{a}\,K\mathrm{p}\Delta P^{1/2} \tag{13.15}$$

where $[H(\mathrm{a})]$, Ka, and Kp represent the amount of adsorbed hydrogen, the square root of the dissociation constant of the adsorbed hydrogen, and the square root of

the adsorption constant of gaseous hydrogen, respectively. Equation 13.12 is the first-order rate equation for this system.

First-order kinetics for the reaction would indicate that the rate-determining step is either the decomposition of hydrogen molecules, or a process whose rate is proportional to $[H(a)]^2$. In the case of Eq. 13.13, the reaction rate is proportional to the concentration of hydrogen atoms that are present at the surface. Equation 13.14 shows the zero-order rate equation, which is a characteristic form of the gas-phase-solid-phase reactions. This relationship indicates that the number of surface atoms of hydrogen which is not influenced by the hydrogen pressure ΔP. The preferred sorption process is therefore one which involves hydrogen adsorption, and even at very low hydrogen pressures the surface is fully covered by hydrogen atoms.

References

1. Flanagan TB, Oates WA (1988) Thermodynamics of intermetallic compound-hydrogen systems. In: Schlapbach L (ed) Hydrogen in intermetallic compounds I. Springer, Berlin, pp 49–85
2. Griessen R, Riesterer T (1988) Heat of formation models. In: Schlapbach L (ed) Hydrogen in intermetallic compounds I. Springer, Berlin, pp 219–284
3. Lynch JF, Reilly JJ (1982) Behavior of H-$LaNi_5$ solid solutions. J Less-Common Met 87: 225–236
4. Osumi Y, Suzuki H, Kato A, Oguro K, Nakane M (1981) Effect of metal-substitution on hydrogen storage properties for mischmetal-nickel alloys. Nippon Kagaku Kaishi 124: 1493–1502
5. Murray JJ, Post ML, Taylor JB (1980) Differential heat flow calorimetry of the hydrides of intermetallic compounds. J Less-Common Met 73:33–40
6. Murray JJ, Post ML, Taylor JB (1983) The thermodynamics of the system $CaNi_5$-H_2 using differential heat conduction calorimetry. J Less-Common Met 90:65–73
7. Post ML, Murray JJ, Taylor JB (1984) Metal hydride studies at the National Research Council of Canada. Int J Hydrogen Energy 9:137–145
8. Post ML, Murray JJ, Grant DM (1989) The $LaNi_5$—H_2 System at T = 358 K: an investigation by heat-conduction calorimetry. Z Phys Chem N F 163:135–140
9. Wenzl H, Lebsanft E (1980) Phase diagram and thermodynamic parameters of the quasibinary interstitial alloy $Fe_{0.5}Ti_{0.5}H_x$ in equilibrium with hydrogen gas. J Phys F 10:2147–2156
10. Murray JJ, Post ML, Taylor JB (1981) The thermodynamics of the $LaNi_5$-H_2 system by differential heat flow calorimetry I: Techniques; the α + β two-phase region. J Less-Common Met 80:201–209
11. Buschow KHJ, van Mal HH (1972) Phase relations and hydrogen absorption in the lanthanum-nickel system. J Less-Common Met 29:203–210
12. Mendelsohn (1977) $LaNi_{5-x}Al_x$ is a versatile alloy system for metal hydride applications. Nature 269:45–47
13. Osumi Y, Suzuki H, Kato A, Nakane M, Miyake Y (1978) Absorption-desorption characteristics of hydrogen for mischmetal based alloys. Nihon Kagaku Kaishi 1472–1477 (in Japanese)
14. Reilly JJ, Wiswall (1974) Formation and properties of iron titanium hydride. Inorg Chem 13:218–222

15. Osumi Y, Suzuki H, Kato A, Nakane M, Miyake Y (1979) Absorption-desorption characteristics of hydrogen for titanium-cobalt alloys. Nihon Kagaku Kaishi 855–860 (in Japanese)
16. Gamo T, Moriwaki Y, Yanagihara N, Yamashita T, Iwaki T (1985) Formation and properties of titanium-manganese alloy hydrides. Int J Hydrogen Energy 10:39–47
17. Ishido Y, Nishimiya N, Suzuki Y (1977) Preparation and equilibrium study on $ZrMn_2H_x$. Denki Kagaku 45:52–54
18. Shaltiel D, Jacob I, Davidov D (1977) Hydrogen absorption properties of AB_2 Laves-phase pseudobinary compounds. J Less-Common Met 53:117–131
19. Chase MW Jr, Davis CA, Downey JR Jr, Frurip DJ, McDonald RA, Syverud AN (1985) J Phys Chem Ref Data 14, Suppl No 1:1266
20. Nomura K, Akiba E, Ono S, Suda S (1979) Kinteics of the reaction between Mg_2Ni and H_2. In: JIMIS-2 Hydrogen in Metals, Minakami, Japan. The Japan Institute of Metals, Sendai, pp 353–356
21. Sandrock GD, Murray JJ, Post ML, Taylor JB (1982) Hydrides and deuteride of $CaNi_5$. Mat Res Bul 17:887–894
22. van Mal HH, Buschow KHJ, Miedcma AR (1974) Hydrogen absorption in $LaNi_5$ and related compounds: experimental observations and their explanation. J Less-Common Met 35:65–76
23. Didisheim JJ, Zolliker P, Yvon K, Fischer P, Schefer J, Gubelmann M, Williams AF (1984) Dimagnesium iron(II) hydride, Mg_2FeH_6, containing octahedral FeH_6^{4-} anions. Inorg Chem 23:1953–1957
24. Zolliker P, Yvon K, Fischer P, Schefer J (1985) Dimagnesium cobalt(I) pentahydride, Mg_2CoH_5, containing square-pyramidal pentahydrocobaltate(4-) (CoH_5^{4-}) anions. Inorg Chem 24:4177–4180
25. Flanagan TB (1978) Thermodynamics of metal, alloy and intermetallic/hydrogen systems. In: Andresen AF, Maeland AJ (eds) Hydrides for energy storage: proceedings of an international symposium, Geilo, August 1977. Oxford, Pergamon, pp 43–59
26. Rudman PS (1979) Hydrogen-diffusion-rate-limited hydriding and dehydriding kinetics. J Appl Phys 50:7195–7199
27. Boulet JM, Gerard N (1983) The mechanism and kinetics of hydride formation in Mg-10 wt% Ni and $CeMg_{12}$. J Less-Common Met 89:151–161
28. Mintz MH, Bloch J (1985) Evaluation of the kinetics and mechanisms of hybriding reactions. Prog Solid State Chem 16:163–194
29. Rudman PS (1983) Hydriding and dehydriding kinetics. J Less-Common Met 89:93–110
30. Sharp JH, Brindley GW, Achar BNA (1966) Numerical data for some commonly used solid state reaction equations. J Am Ceram Soc 49:379–382
31. Hancock JD, Sharp JH (1972) Method of comparing solid-state kinetic data and its application to the decomposition of Kaolinite, Brucite and $BaCO_3$. J Am Ceram Soc 55:74–77